Supporting Information

Temperature-dependent Mechanochromic Behavior of Mechanoresponsive Luminescent Compounds

Yoshimitsu Sagara,* Kazuya Kubo, Takayoshi Nakamura, Nobuyuki Tamaoki, and Christoph Weder*

E-mail: sagara@es.hokudai.ac.jp; christoph.weder@unifr.ch

Table of Contents

General methods and materials S2
Synthesis of compound **1** S2
Thermogravimetric analysis (TGA) of **1** in the Y-form S4
Photoluminescence color changes of **1** induced by various stimuli S4
Characterization of the RO-form S5
Differential Scanning Calorimetry (DSC) traces S6
Absorption spectrum of **1** in chloroform S6
Emission lifetime and quantum yields measurements S7
XRD and emission spectra showing the transition from the Am- to the YG-from S8
Images and XRD spectra showing the direct transition from the Y- to the YG-form S9
Temperature-dependent MRL behavior of **2** S9
Single crystal structure of **1** in the Y-form S10
References S11

General methods and materials

All reagents and solvents were purchased from Aldrich and Tokyo Kasei. Unless otherwise noted, all reactions were carried out under nitrogen atmosphere. Silica gel column chromatography was carried out with silica gel from Kanto Chemicals (silica gel 60 N, spherical, 63-210 μm). ^{1}H NMR spectra were recorded on a JEOL JNM-ECX 400 spectrometer and all chemical shifts are quoted on the δ-scale in ppm relative to the signal of tetramethylsilane (at 0.00) as an internal standard. Proton-decoupled ^{13}C NMR spectra were recorded on a JEOL JNM-ECX 400 spectrometer and all chemical shifts (δ) are reported in ppm using residual solvent as the internal standard ($CDCl_3$ at 77.16). Coupling constants (J) are reported in Hz and relative intensities are also shown. Matrix-assisted laser desorption ionization time-of-flight (MALDI-TOF) mass spectra were obtained on an AB SCIEX TOF/TOF 5800. Elemental analysis was carried out with an Exeter Analytical CE440 Elemental Analyzer. The DSC measurements were conducted using a Rigaku Thermo plus EVO DSC8230 with a heating/cooling rate of 10 ˚C/min under nitrogen atmosphere. The thermogravimetric analysis was conducted using a Rigaku Thermo plus TG8120 under nitrogen. Powder X-ray diffraction measurements were carried out with a Rigaku SmartLab. UV-vis absorption spectrum was measured with a JASCO V-550. Steady-state fluorescence spectra were recorded on a JASCO FP-6500. The solid samples for steady-state fluorescence spectra were carefully sandwiched between quartz substrates and were set in the sample chamber of the fluorometer so that the detector gathers fluorescence from the surface of the sandwiched solid. Time-resolved fluorescence measurements were carried out with a Hamamatsu Photonics Quantaurus-Tau. Quantum efficiencies were measured with a Hamamatsu Photonics Quantaurus-QY. Single crystal data was collected with Cu-Kα radiation (λ = 1.54187 Å) at 293 K using a Rigaku MicroMax-007HF diffractometer with Pilatus 200K. The crystal was mounted on a glass needle and all geometric and intensity data were taken from this crystal. The structure was solved and refined by full-matrix least-squares techniques on F^2 with the Crystal structure software package and Yadokari-XG.[S1,S2] All atoms (except hydrogen atoms) were refined anisotropically. Hydrogen atoms were introduced at residual electronic density positions observed near their expected positions. The X-ray crystallographic file for **1** was deposited in the Cambridge Crystallographic Data Centre (CCDC) (deposition code: CCDC 1476838). The CIF file can be obtained free of charge from the CCDC via www.ccdc.cam.ac.uk/data_request/cif.

Synthesis of compound 1

The synthetic route used to prepare compound **1** is shown in Scheme S1. 4-(6-Bromohexyloxy)benzyl cyanide was prepared according to the previously reported procedure.[S3]

Scheme S1

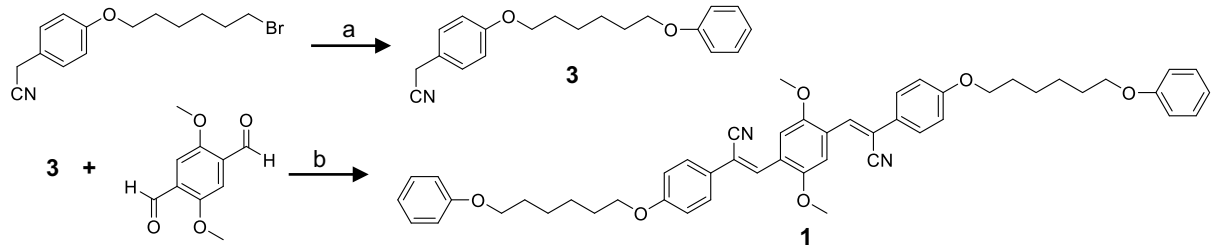

Conditions: (a) phenol, K_2CO_3, DMF, 60 °C, 3 h; (b) *t*-BuOK, *n*-Bu_4NOH, *i*-PrOH, THF, 50 °C, 45 min.

4-(6-Phenoxyhexyloxy)benzyl cyanide (3). A mixture of 4-(6-bromohexyloxy)benzyl cyanide (1.00 g, 3.38 mmol), phenol (349 mg, 3.71 mmol) and K_2CO_3 (1.40 g, 10.1 mmol) in DMF (70 mL) was vigorously stirred for 3 h at 60 °C, before it was cooled to room temperature and poured into ethyl acetate. The resulting mixture was washed with saturated aqueous NH_4Cl solution (4 × 100 mL) and saturated aqueous NaCl solution (1 × 100 mL) and subsequently dried over $MgSO_4$, before the solvent was evaporated. The crude product was purified by flash column chromatography on silica gel (eluent: hexane/ethylacetate = 1:4) and subsequent re-precipitation (dichloromethane/methanol) to afford compound **3** (692 mg, 2.24 mmol) as a white powder in 66% yield.
^{1}H NMR (400 MHz, $CDCl_3$): δ = 1.52–1.56 (m, 4H), 1.79–1.84 (m, 4H), 3.68 (s, 2H), 3.95–3.99 (m, 4H), 6.88–6.96 (m, 4H), 7.22 (d, J = 8.8 Hz, 2H), 7.26–7.30 (m, 2H). ^{13}C NMR (100 MHz, $CDCl_3$): δ = 20.91, 25.94, 25.98, 29.24, 29.32, 67.73, 68.04, 114.56, 115.15, 118.37, 120.62, 121.67, 129.15, 129.53, 158.94, 159.14. MS (MALDI-TOF): m/z: 332.21 (calcd. $[M + Na]^+$ = 332.16).

1,4-Bis(α-cyano-4-(6-phenoxyhexyloxystyryl))-2,5-dimethoxybenzene (1). A suspension of **3** (600 mg, 1.94 mmol) and 2,5-dimethoxybenzene-1,4-dicarboxaldehyde (184 mg, 0.946 mmol) in a mixture of THF (20 mL) and *i*-PrOH (100 mL) was prepared by stirring at 50 °C. Then, *n*-Bu_4NOH (1.9 mL of 1 M solution in methanol) and *t*-BuOK (0.19 mL of 1 M solution in THF) were quickly added and the reaction mixture was stirred for 45 min at 50 °C. Methanol (30 mL) was added, the reaction mixture was allowed to cool to room temperature, and the resulting precipitate was filtered off. The crude product was washed with methanol containing several drops of acetic acid (2 × 100 mL) and pure methanol (2 × 100 mL) before it was purified by re-precipitation (chloroform/hexane) to afford compound **1** (643 mg, 0.828 mmol) as a yellow powder in 87% yield.
^{1}H NMR (400 MHz, $CDCl_3$): δ = 1.55–1.59 (m, 8H), 1.80–1.87 (m, 8H), 3.95 (s, 6H), 3.99 (t, J = 6.4 Hz, 4H), 4.03 (t, J = 6.4 Hz, 4H), 6.89–6.97 (m, 10H), 7.26–7.31 (m, 4H), 7.64 (d, J = 8.8 Hz, 4H), 7.88 (s, 2H), 7.89 (s, 2H). ^{13}C NMR (100 MHz, $CDCl_3$): δ = 25.95, 26.00, 29.23, 29.33, 56.44, 67.73, 68.14, 110.23, 111.59, 114.56, 115.03, 118.69, 120.63, 125.49, 127.04, 127.57, 129.53, 133.77, 151.93, 159.14, 160.14. MS (MALDI-TOF): m/z: 776.50 (calcd. $[M]^+$ = 776.38). Elemental analysis (%) calcd. for $C_{50}H_{52}N_2O_6$: C 77.29, H 6.75, N 3.61; found: C 77.25, H 6.72, N 3.59.

Thermogravimetric analysis (TGA) of 1 in the Y-form

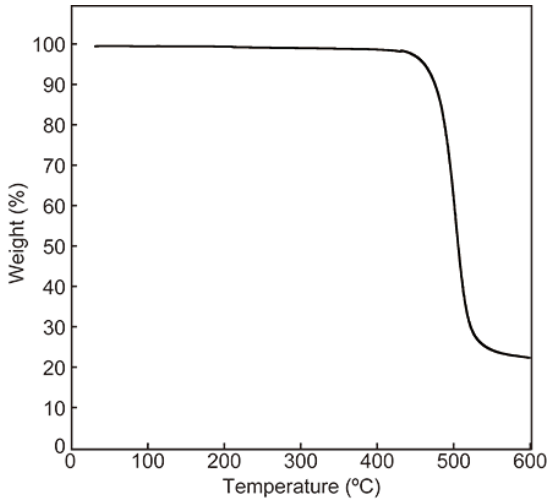

Figure S1. TGA curve acquired for the Y-form of compound **1**. The measurement was conducted under N_2.

Photoluminescence color changes of 1 induced by various stimuli

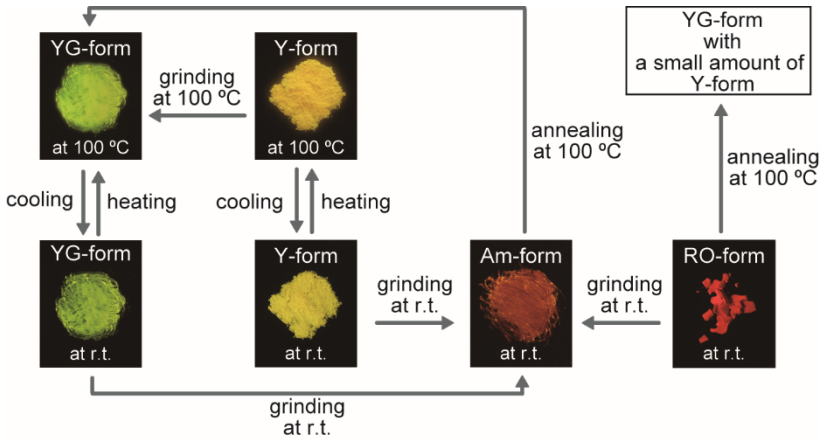

Figure S2. Pictures showing the photoluminescence color changes of compound **1** as a result of various thermal and/or mechanical stimuli. All images were taken on quartz substrates under UV light excitation (365 nm).

Characterization of the RO-form

Compound **1** can be isolated in another ordered state by precipitation from a chloroform solution into methanol; this process afforded a material displaying reddish-orange photoluminescence (RO-form). X-ray diffraction measurements confirm that the RO-form is also an ordered state and the diffraction pattern differs from those of the Y-form and the YG-form (Figure S3, red line). Thus, compound **1** forms three different ordered forms and one amorphous form. Given that cyano-OPV derivatives with plain alkyl chains in the peripheral positions have never been reported to form more than two molecular assembled states, the introduction of phenyl group appears to be key for inducing additional (meta)stable molecular assembled states. The peak of the broad emission spectrum of the RO-form appears at 650 nm (Figure S4) and the long lifetime of 36.7 ns (Table S1) indicates that the reddish-orange photoluminescence is associated with excimer formation. Annealing of the RO-form at 100 °C for 30 min leads to a transition to the YG-form. This transition was confirmed by changed XRD patterns as shown in Figure S3. The obtained diffractogram is very similar to that of the YG-form. However, in the emission spectra (Figure S4), a shoulder characteristic of the YG-form is not clearly seen after the thermal treatment, suggesting that a portion of the RO-form transforms into the Y-form and that energy transfer from the YG-form to the Y-form is at play. The DSC curve of the RO-form of **1** displays one exothermic peak at 88.2 °C (Figure S5), suggesting that the RO-form is a thermodynamically metastable state.

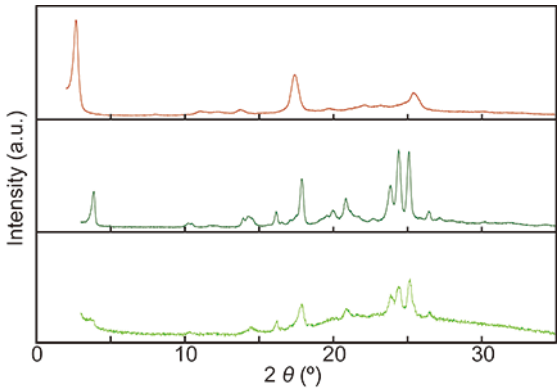

Figure S3. XRD patterns of the RO-form (yellow line) of compound **1**, the RO-form after annealing at 100 °C for 30 min (dark green line), and the YG-form (green line). All measurements were carried out at room temperature.

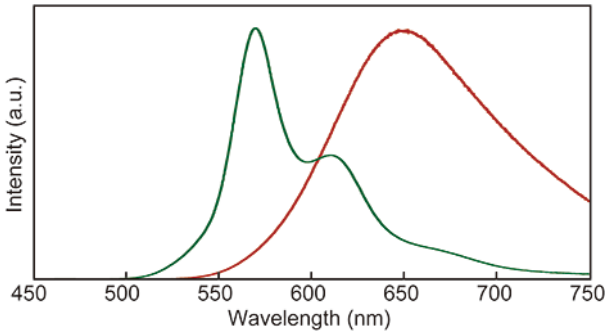

Figure S4. Photoluminescence spectra of the RO-form (red solid line) and the RO-from after annealing at 100 °C for 30 min (deep green line). All measurements were carried out at room temperature. λ_{ex} = 400 nm.

Differential Scanning Calorimetry (DSC) traces

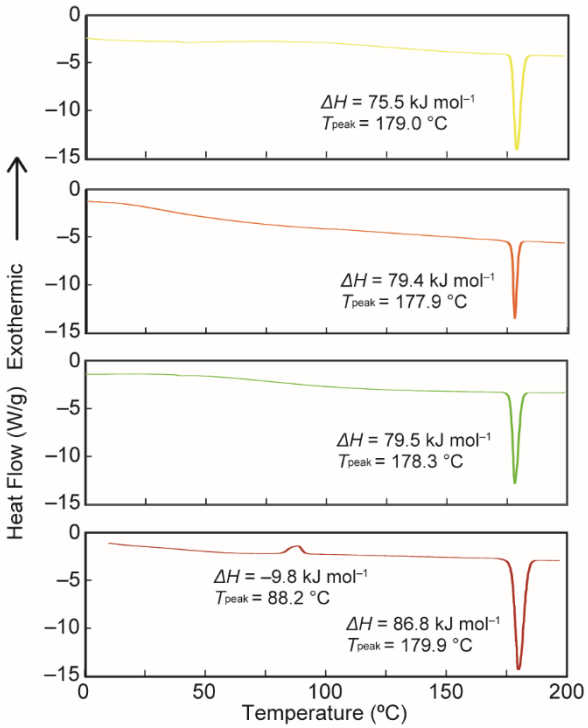

Figure S5. First heating DSC traces of the Y-form (yellow line), the Am- form (orange line), the YG-form (green line), and the RO-form (red line) of compound **1**.

Absorption spectrum of 1 in chloroform

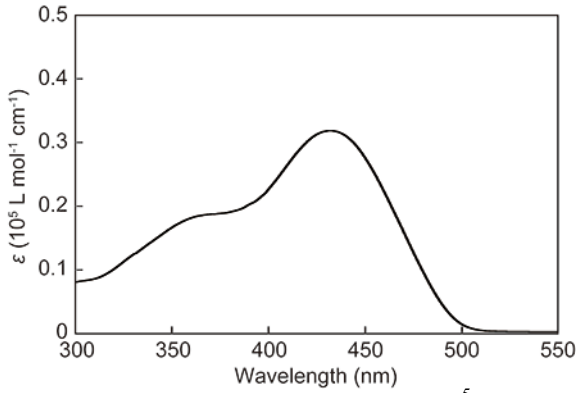

Figure S6. Absorption spectrum of compound **1** in chloroform ($c = 1 \cdot 10^{-5}$ M).

Emission lifetime and quantum yields measurements

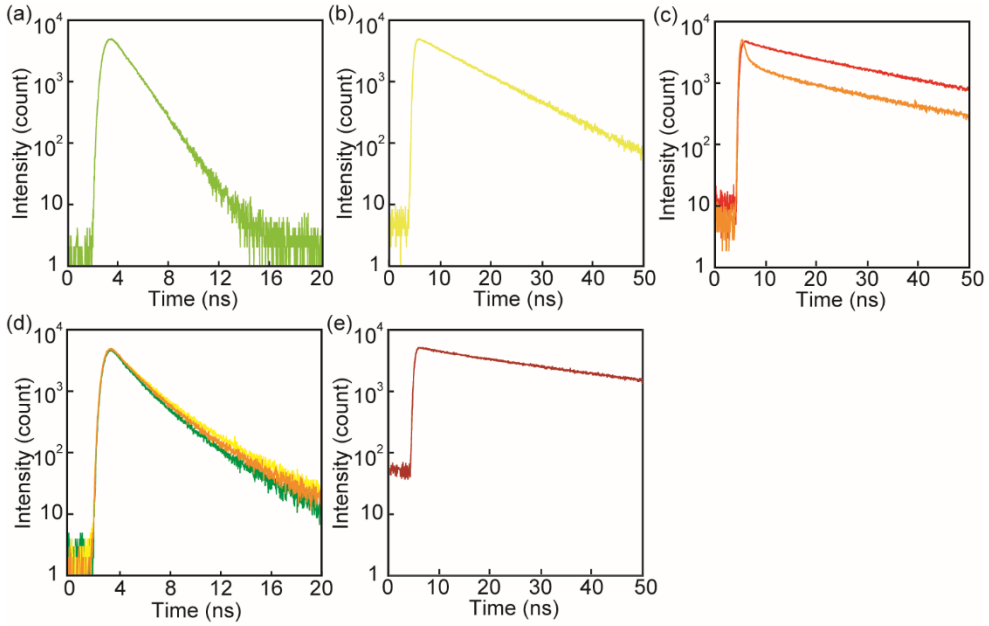

Figure S7. Emission decay curves of a dilute chloroform (c = ca. 1×10^{-6} M) solution (a, monitored at 540 nm), the Y-form (b, monitored at 570 nm), the Am-form (c, monitored at 570 and 650 nm), the YG-form (d, monitored at 530, 570, and 620 nm), and the RO-form (e, monitored at 650 nm) of compound **1**. All measurements were carried out at room temperature. λ_{ex} = 405 nm.

Table S1. Emission lifetimes and emission quantum yields of the different forms of compound **1**.[a]

	τ_i(amplitude a_i) (ns)	X^2	Φ_{PL}
1 in chloroform monitored at 540 nm	1.4 (100%)	1.00	0.42
Y-form monitored at 570 nm	9.7 (100%)	1.03	0.65
Am-form monitored at 570 nm	0.3 (69%), 1.1 (14%), 5.0 (5%), 25.3 (12%)	1.04	0.39
at 650 nm	1.4 (14%), 7.8 (10%), 25.7 (76%)	1.09	
YG-form monitored at 530 nm	1.1 (65%), 2.8 (35%)	1.01	0.38
at 570 nm	1.3 (65%), 3.3 (35%)	1.01	
at 620 nm	1.2 (64%), 2.9 (36%)	1.06	
RO-form monitored at 650 nm	4.5 (11%), 36.7 (89%)	1.01	0.25

[a] All measurements were carried out at room temperature.

XRD and emission spectra showing the transition from the Am- to the YG-from

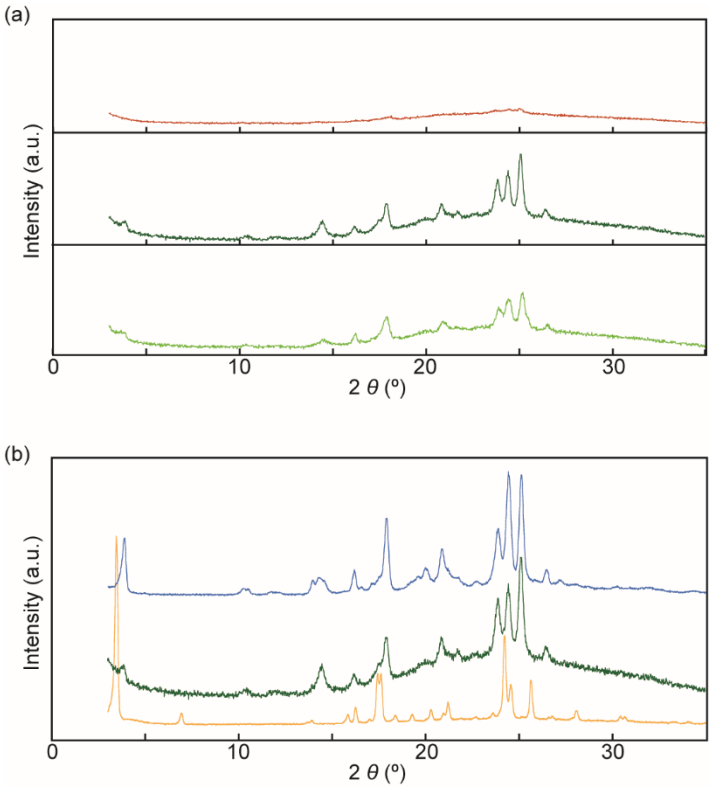

Figure S8. (a) XRD patterns of the Am-form made from the Y-form (red line), the annealed Am-form (dark green line), and the YG-form (green line) of compound **1**. (b) Comparison of the XRD patterns of the sample prepared through thermal treatment to the RO-form (blue line, same data as shown in Figure S3), the YG-form obtained through annealing to the Am-form (dark green line, same data as shown in panel (a)), and the Y-form (yellow line, same data as shown in Figure 2) of compound **1**. All measurements were carried out at room temperature.

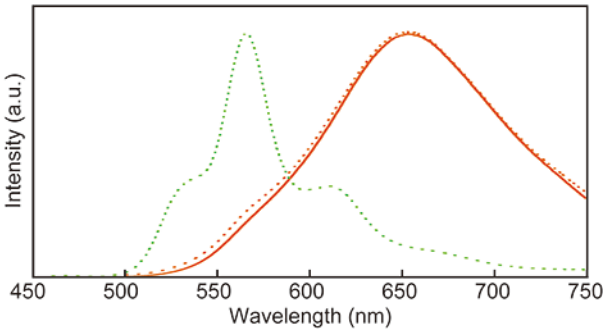

Figure S9. Photoluminescence spectra of the Am-form made from the Y-form (red solid line) of compound **1**, the annealed Am-from (green dotted line), and the Am-form made by grinding the latter at room temperature (red dotted line). All measurements were carried out at room temperature. λ_{ex} = 400 nm.

Images and XRD spectra showing the direct transition from the Y- to the YG-form

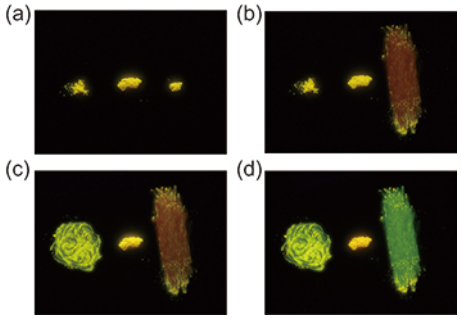

Figure S10. Images representing changes of the photoluminescence color upon grinding the Y-form of **1** at 50 °C. (a) Three piles of **1** in the Y-form are placed on a quartz substrate and pictured while heated at 50 °C. (b) The right portion was vigorously ground at 50 °C. (c) Subsequently, the left portion was gently ground at 50 °C. (d) The samples were heated to 100 °C. All images were taken on quartz substrates under UV light excitation (365 nm).

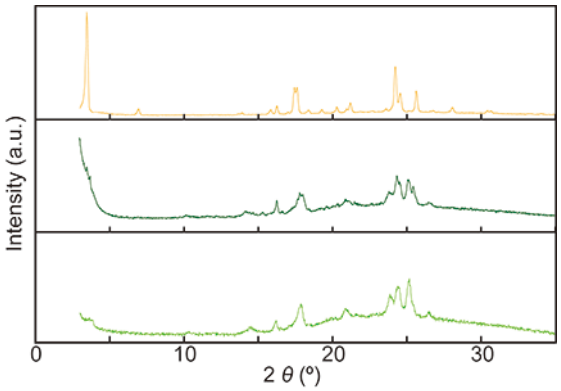

Figure S11. XRD patterns of the Y-form (yellow line), the Y-form after gentle grinding at 50 °C (dark green line), and the YG-form (green line). All measurements were carried out at room temperature.

Temperature-dependent MRL behavior of 2

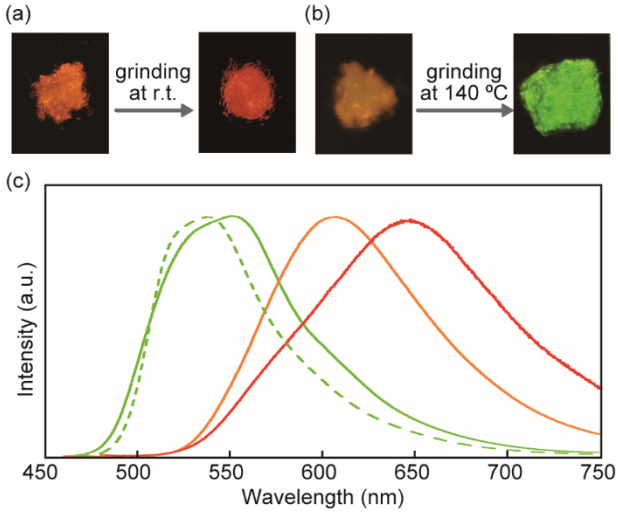

Figure S12. (a,b) Images documenting the mechanically induced photoluminescence changes of compound **2** at room temperature and 140 °C. The images were taken on quartz substrates under excitation light at 365 nm at room temperature and at 140 °C, respectively. (c) Photoluminescence spectra of the orange-emitting form (orange solid line), the sample after grinding at room temperature (red solid line), the sample after grinding at 140 °C (green solid line) and the green-emitting crystals obtained from recrystallization (green dotted line). All spectra were measured at room temperature. λ_{ex} = 400 nm.

Single crystal structure of 1 in the Y-form

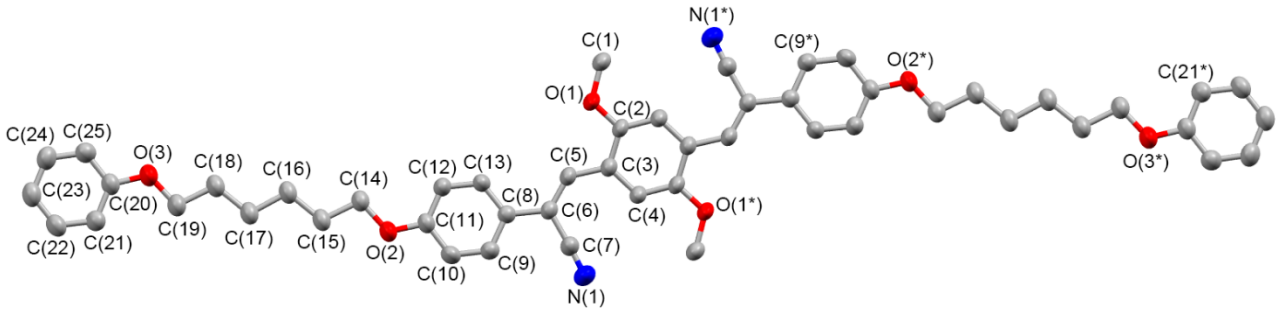

Figure S13. Molecular view of **1** in the Y-form; Ellipsoids are drawn at 50 % of probability; *: 3-x,-y,-z. Hydrogen atoms are omitted for clarity.

Table S2. Crystal data and structure refinement for **1** in the Y-form.

Empirical formula	$C_{50}H_{52}N_2O_6$
Formula weight	776.93
Temperature	293(2) K
Wavelength	1.54187 Å
Crystal system	monoclinic
Space group	$P2_1/c$
Unit cell dimensions	a = 7.4921(11) Å
	b = 5.4706(9) Å
	c = 50.810(7) Å
	β = 83.941(12)°
Volume	2082.3(5) Å^3
Z	2
Density (calculated)	1.239 Mg/m^3
Absorption coefficient	0.643 mm^{-1}
F(000)	828
Crystal size	0.210 x 0.160 x 0.030 mm^3
Theta range for data collection	6.903 to 74.710°.
Index ranges	-9<=h<=8, -6<=k<=6, -63<=l<=60
Reflections collected	16024
Independent reflections	4011 [R(int) = 0.0772]
Completeness	0.938
Goodness-of-fit on F^2	0.905
Final R indices [I>2sigma(I)]	$R1$ = 0.0581, w$R2$ = 0.1322
R indices (all data)	$R1$ = 0.0721, w$R2$ = 0.1364
Extinction coefficient	0.0150(11)

References

(S1) Kabuto, C.; Akine, S.; Nemoto, T.; Kwon, E. *J. Cryst. Soc. Jpn.* **2009**, *51*, 218–224.

(S2) (a) Burla, M. C.; Caliandro, R.; Carrozzini, B.; Cascarano, G. L.; Giacovazzo, C.; Mallamo, M.; Mazzone, A.; Polidori, G. In preparation, http://wwwba.ic.cnr.it/content/sir2011-v10; (b) Sheldrick, G. M. SHELXL-2014/7 Programs for Crystal Structure Analysis, Universitat Göttingen, Göttingen, Germany, http://shelx.uni-ac.gwdg.de/SHELX/index.php.

(S3) Sagara, Y.; Lavrenova, A.; Crochet, A.; Simon, Y. C.; Fromm, K. M.; Weder, C. *Chem. Eur. J.* **2016**, *22*, 4374–4378.